Antiviral Research 192 (2021) 105115

Contents lists available at ScienceDirect

Antiviral Research

journal homepage: www.elsevier.com/locate/antiviral

# Selinexor, a novel selective inhibitor of nuclear export, reduces SARS-CoV-2 infection and protects the respiratory system *in vivo*

Trinayan Kashyap [a,1], Jackelyn Murray [b,1], Christopher J. Walker [a], Hua Chang [a], Sharon Tamir [a], Bing Hou [c], Sharon Shacham [a], Michael G. Kauffman [a], Ralph A. Tripp [b,2], Yosef Landesman [a,*,2]

[a] Karyopharm Therapeutics, Newton, MA, USA
[b] University of Georgia College of Veterinary Medicine, Athens, GA, USA
[c] Antengene Corporation Co., Ltd., Shaoxing, PR China

ARTICLE INFO

*Keywords:*
Exportin-1
XPO1
CRM1
SARS-CoV-2
COVID19
Selinexor
SINE compound

ABSTRACT

The novel coronavirus disease 2019 (COVID-19) caused by the severe acute respiratory syndrome coronavirus 2 (SARS-CoV-2) is responsible for the recent global pandemic. The nuclear export protein (XPO1) has a direct role in the export of SARS-CoV proteins including ORF3b, ORF9b, and nucleocapsid. Inhibition of XPO1 induces anti-inflammatory, anti-viral, and antioxidant pathways. Selinexor is an FDA-approved XPO1 inhibitor. Through bioinformatics analysis, we predicted nuclear export sequences in the ACE-2 protein and confirmed by *in vitro* testing that inhibition of XPO1 with selinexor induces nuclear localization of ACE-2. Administration of selinexor inhibited viral infection prophylactically as well as therapeutically *in vitro*. In a ferret model of COVID-19, selinexor treatment reduced viral load in the lungs and protected against tissue damage in the nasal turbinates and lungs *in vivo*. Our studies demonstrated that selinexor downregulated the pro-inflammatory cytokines IL-1β, IL-6, IL-10, IFN-γ, TNF-α, and GMCSF, commonly associated with the cytokine storm observed in COVID-19 patients. Our findings indicate that nuclear export is critical for SARS-CoV-2 infection and for COVID-19 pathology and suggest that inhibition of XPO1 by selinexor could be a viable anti-viral treatment option.

## 1. Introduction

Infection with severe acute respiratory syndrome coronavirus 2 (SARS-CoV-2) results in coronavirus disease 19 (COVID-19), a respiratory illness that was first identified in Wuhan, China in December 2019 and led to a global pandemic (Gandhi et al., 2020; Lai et al., 2020). The clinical manifestation of SARS-CoV-2 can range from mild to severe symptoms which include fever, cough, sore throat, acute respiratory distress syndrome, viral pneumonia, and respiratory failure (Gandhi et al., 2020). Patients with COVID-19 can develop dysregulation of the immune system and immune overactivation (i.e., cytokine storm), which are strong contributing factors to COVID-19-linked deaths (Ingraham et al., 2020). The novel coronavirus SARS-CoV-2 is most closely related to the SARS-CoV virus that caused an epidemic in 2002, and both viruses are members of the B lineage of the *Betacoronaviruses* genus (Shereen et al., 2020; Zhu et al., 2020). SARS-CoV-2 infection is facilitated by the binding of the viral S protein to the host cellular receptor angiotensin-converting enzyme 2 (ACE-2) and requires accessory cell surface proteases such as the serine proteases TMPRSS2 and ADAM17 (Heurich et al., 2014; Shereen et al., 2020).

Selective inhibitors of nuclear export (SINE) are a class of small molecules that have demonstrated broad spectrum anti-viral and anti-inflammatory properties (Widman et al., 2018). Nuclear export protein exportin-1 (XPO1), also called Chromosome Region Maintenance 1 (CRM1), is part of the karyopherin-β superfamily of nuclear transport proteins, which includes 15 different importin and exportin proteins (Perwitasari et al., 2016). SINE compounds specifically inhibit XPO1, resulting in nuclear sequestration of XPO1-dependent cargo proteins (Sun et al., 2013; Widman et al., 2018).

Selinexor is a potent, oral, slowly reversible SINE small molecule drug that binds covalently to XPO1 and blocks the shuttling of XPO1 cargo proteins from the nucleus to the cytoplasm. XPO1 inhibitors have demonstrated activity against over 20 different viruses, including DNA and RNA viruses like influenza and respiratory syncytial virus (RSV) that

* Corresponding author. Karyopharm Therapeutics, 85 Wells Avenue, Newton, MA, 02459, USA.
*E-mail address:* ylandesman@karyopharm.com (Y. Landesman).
[1] Equal contribution.
[2] Co-senior authors.

https://doi.org/10.1016/j.antiviral.2021.105115
Received 28 May 2021; Accepted 1 June 2021
Available online 19 June 2021

cause respiratory infections (Jorquera et al., 2019; Perwitasari et al, 2014, 2016; Widman et al., 2018). More than 200 XPO1 cargo proteins have been identified including proteins with regulatory roles in cell growth, differentiation, and inflammatory response (Lee et al., 2020). In addition, XPO1 cargo proteins include many viral proteins such as the Rev protein of HIV (Cao et al., 2009), NEP of influenza (Paragas et al., 2001), and agnoprotein of the JC virus (Saribas et al., 2020), for which their bidirectional shuttling between nucleus and cytoplasm is essential for viral propagation. Importantly, XPO1 has a direct role in SARS-CoV replication and pathogenesis, and is responsible for the nuclear export of certain SARS-CoV proteins including ORF3b (Freundt et al., 2009; Konno et al., 2020), ORF9b (Jiang et al., 2020; Moshynskyy et al., 2007; Sharma et al., 2011; Shi et al., 2014) and nucleocapsid N protein (Li et al., 2020; Timani et al., 2005; You et al., 2007). These proteins help the virus evade innate immunity by inhibiting induction of type I interferon (Freundt et al., 2009; Jiang et al., 2020; Konno et al., 2020; Kopecky-Bromberg et al., 2007; Li et al., 2020). Similar activity was also reported for the host nuclear protein glioma tumor suppressor candidate region gene 2 (GLTSCR2), as coronavirus infection induces XPO1-dependent cytoplasmic translocation of GLTSCR2, leading to attenuated IFN-β induction and supporting viral replication (Li et al., 2017; Wang et al., 2016).

Selinexor and other SINE compounds have demonstrated potent anti-inflammatory activity through the inhibition of NF-κB (Kashyap et al., 2016), leading to reductions in cytokines such as IL-6, IL-1 and IFN-γ. In addition, inhibition of XPO1 leads to the activation of several anti-inflammatory, antioxidant, and cytoprotective transcription factors including IκB, PPARγ (Umemoto and Fujiki, 2012), RXRα (Prüfer and Barsony, 2002), HMGB1 (Hyun et al., 2016), COMMD1 (Muller et al., 2009), and Nrf2 (Tajiri et al., 2016). An example of the potent anti-inflammatory activity of selinexor was demonstrated in a mouse model of sepsis (induced by a lethal dose of lipopolysaccharide), where oral selinexor treatment increased survival and reduced inflammatory cytokine secretion while reducing the numbers of macrophage and polymorphonuclear neutrophils in the peritoneal cavity (Wu et al., 2018). In this mouse sepsis model, selinexor treatment attenuated the acute respiratory distress syndrome-like lung injury. These findings are significant as COVID-19 severity correlates with circulating cytokine levels in patients (Wu et al., 2018).

Recently, three studies suggested a central role for XPO1 and the SINE drugs in COVID-19. The first study discovered that XPO1 and three other host hub proteins have the highest number of functional connections with the SARS-CoV-2 viral proteins (Zhou et al., 2020). The second study mapped the SARS-CoV-2 protein-protein interaction map and suggested to repurpose the SINE drug verdinexor as a treatment for COVID-19 based on *in vitro* studies showing the ability of verdinexor to inhibit specific viral-host protein interactions (Gordon et al., 2020). In a third study, selinexor was ranked 18 out of 400 drugs screened in terms of drugs whose effects negate the master regulator proteins induced by SARS-CoV-2 infection (Laise et al., 2020). Blockade of XPO1 is therefore expected to inhibit viral assembly and propagation (Uddin et al., 2020). Here, we provide an *in vitro* and *in vivo* analysis of the efficacy of selinexor on the modulation of the anti-viral and the anti-inflammatory effects of selinexor in the context of SARS-CoV-2.

## 2. Materials and methods

### 2.1. Nuclear export signal (NES) prediction

Predictions of NESs were performed using NetNES 1.1(la Cour et al., 2004) and Wregex v2.2 (Prieto et al., 2014). Wregex queries were performed for the leucine-rich NES binding to the CRM1 protein with recommended settings. An overall prediction score was assigned based on both algorithms using a threshold of 0.5 for NetNES and 50 for Wregex (strongly indicates both predictions exceed the thresholds, and moderately indicates that only one algorithm exceeds the thresholds).

### 2.2. Anti-viral in vitro efficacy assays

SARS-CoV-2 (2019-nCoV/USA-WA1/2020; MN985325.1) was received from BEI resources. Viral neutralization assays were performed for SARS-CoV-2. Vero E6 cells (ATCC: #CRL-1586) cultured in DMEM with 10% fetal bovine serum (FBS) were incubated overnight at 8 x $10^5$ cells per well in a 6-well plate. Cells were washed and media was FBS containing SARS-CoV2. Cells were infected at multiplicity of infection (MOI) of 0.01 for 1 h. Following infection, selinexor was added at concentrations of 0, 10, 30, and 100 nM to the wells in 2X overlay in DMEM with 1.2% Avicel® supplemented with 1% FBS at 0, 24, 36 and 48 h. Total infection time was 4 days at 37 °C, 5% $CO_2$. At the end of the experiment, cells were fixed for 20 min with acetone and methanol (60:40) and stained by crystal violet in order to count plaques and calculate viral titer (PFU/ml). The virus was only propagated once and never passaged.

Vero E6 cells were plated on glass coverslips (BioCoat, BD Biosciences) at 500,000 cells/well in 6-well plates and grown overnight. The following day, the adherent cells were treated with 500 nM selinexor for 24 h. After treatment, coverslips were washed with 1X PBS (phosphate buffered saline) then fixed with 3% PFA and permeabilized/blocked with 0.1% Tween X-100 and 1% BSA (w/v) in PBS. Cells were incubated overnight with ACE2 antibody (Invitrogen, #MA5-32307) diluted 1:50 in 1%BSA/1X PBS. A rabbit secondary antibody, Alexa Fluor 488, green-fluorescent dye (Thermo Fisher, #A11008) was used for all staining, while nuclei were stained with DAPI (Invitrogen). Protein localization was visualized using an Echo Revolve microscope at 60× magnification.

For nuclear/cytoplasmic protein fractionation, Vero E6 cells were treated with 500 nM selinexor for 24 h. Cells were trypsinized, washed with PBS and cellular fractionation was carried out using the NE-PER nuclear and cytoplasmic extraction kit (Thermo Scientific#78833) according to the manufacturer's instructions. Fractionation efficiency was evaluated by protein expression of subcellular marker proteins; Beta-Tubulin (cytoplasmic) and Lamin B (nuclear).

### 2.3. In vivo efficacy studies

The *in vivo* studies were performed by Viroclinics Biosciences B.V. Xplore at their animal facility in Schaijk, The Netherlands under conditions that meet the standard of Dutch law for animal experimentation (2010/63/EU) and are in agreement with the "Guide for the care and use of laboratory animals" (8th edition, NRC 2011), ILAR recommendations, AAALAC standards. The strain of SARS-CoV-2 utilized in the studies was BetaCoV/Munich/BavPat1/2020. Ferrets (*Mustela putorius furo*) were obtained from a dedicated certified supplier in Denmark and were housed by group in an isolator under BSL3 conditions for the duration of the experiment. Group 3 and 4 (placebo) were housed together in one isolator. For intranasal administration and euthanasia by exsanguination, the animals were anesthetized with an intramuscular (i.m) injection of ketamine (20 mg/kg; i.m.) and medetomidine (0.1 mg/kg; i.m.). Atipamezole (0.25 mg/kg; i.m.) was used to antagonize the sedation with medetomidine.

Serologically pre-screened, SARS-CoV-2 negative female ferrets were infected intranasally on day 0 with $10^6$ SARS-CoV-2 $TCID_{50}$/ml (50% tissue culture infective dose/ml). Four hours post-infection, animals received the first oral treatment of either selinexor (5 mg/kg) or placebo (vehicle only) and were treated twice daily (every 12 h) for 3 days. On day 4, animals were euthanized and quantitative PCR was performed on total RNA that was isolated postmortem from the animals' lungs (Corman et al., 2020). Primers and probes specific for beta coronavirus E gene were used (REF): Primers, F:ACAGGTACGTTAATAGTTAATAGCGT; R: ATATTGCAGCAGTACGCACACA; Probe, E_Sarbeco_P1: ACACTAGCCATCCTTACTGCGCTTCG. The number of virus copies in the samples were calculated using the resulting Ct value for the sample against slope, intercept, and upper and lower limits of detection for the

**Table 1**
Predicted nuclear export sequences (NESs) of human host and SARS-CoV-2 proteins.

| Protein | Sequence | Wregex score | NetNES score | Overall Prediction | Published XPO1-Protein Interaction |
|---|---|---|---|---|---|
| Human host proteins | | | | | |
| **ACE-2** | QEIQNLTVKLQLQALQ | 75.0 | 0.62 | Strong | . |
| | EAGQKLFNMLRLGKSE | 64.9 | 0.31 | moderate | . |
| **ADAM17** | LDSLLSDYDI | 63.1 | 0.49 | moderate | . |
| | MLSSMDSASV | 39.8 | 0.62 | moderate | . |
| **TMPRSS2** | LGTFLVGAALA | 43.3 | 1.17 | moderate | . |
| **GLTSCR2** | EAEKLERQLALPATE | 85.8 | 0.46 | moderate | Wang (2016) |
| **IκBα** | MVKELQEIRL | 63.1 | 0.52 | strong | Johnson et al. (1999) |
| **SARS-CoV/2 proteins** | | | | | |
| **Nucleocapsid protein** | LLLLDRLNQLESMSGK | . | 0.98 | moderate | Timani (2005), You (2007) |
| **ORF3b Protein** | IITLKKRWQLAL | 35.1 | 0.655 | moderate | Freundt (2009) |
| **ORF6 Protein** | | . | | weak | . |
| **ORF9b Protein** | . | . | 0.85 | moderate | Moshynskyy (2007), Sharma (2011) |
| **Spike glycoprotein** | SRLDKVEAEVQID | 58.8 | . | moderate | . |
| | SFIEDLLFNKVTLAD | 54.1 | 0.29 | moderate | . |

standard virus included in each run. Levels of infectious (replication competent) virus in the tissues were measured using a virus titration assay on MDCK cells. Data are expressed as Log10 virus particles (CP)/g and Log10 50% tissue culture infectious dose (TCID50)/g, respectively.

Histopathological analysis from selected tissues was performed blinded, for all animals that were euthanized on day 4 post infection. Samples were stored for two weeks in 10% formalin to fully inactivate any virus present prior to sample processing. Sections from the cranial and caudal lung lobes (n = 6 each experimental group; n = 3 control group) and left nasal turbinate were embedded in paraffin and the tissue sections were stained with haematoxylin and eosin (HE) for histological examination. Severity of alveolitis, bronchitis, bronchiolitis, and rhinitis were scored according to the following: 0 = no inflammatory cells, 1 = few inflammatory cells, 2 = moderate number of inflammatory cells, 3 = many inflammatory cells. The extent of alveolitis was scored as 0 = 0%, 1 = <25%, 2 = 25–50%, 3 = >50%. A section of these tissues were homogenized and subjected to Taqman PCR and virus titration.

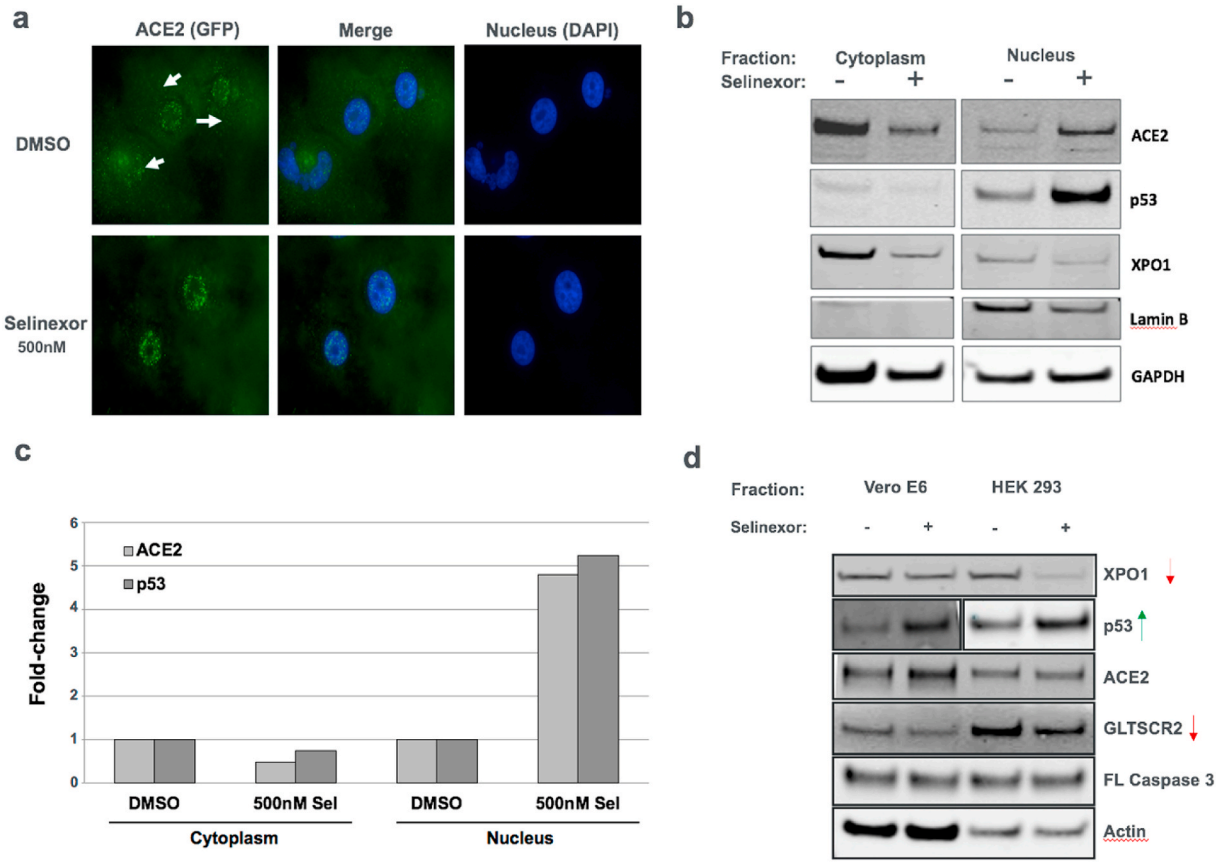


**Fig. 1. Selinexor inhibits nuclear export and forces nuclear accumulation of ACE-2 *in vitro*.** Vero E6 cells were incubated with 500 nM selinexor or DMSO for 24 h. **a)** Cells were fixed with 3% paraformaldehyde, incubated with anti-ACE-2 antibody (Invitrogen, #MA5-32307) followed by a rabbit secondary antibody, Alexa Fluor 488, green-fluorescent dye (Thermo Fisher, #A11008), then visualized with the Echo Revolve fluorescent microscope (ECHO) at 60× magnification. Membrane-bound ACE-2 receptors are present in DMSO-treated cells only (white arrows). **b)** Sub-cellular fractionation was performed post-treatment then analyzed by immunoblots and **c)** quantified by densitometric analysis. **d)** Vero E6 and HEK 293 cells were treated with selinexor (550 nM, 24 h) and whole protein lysates were analyzed on immunoblots.

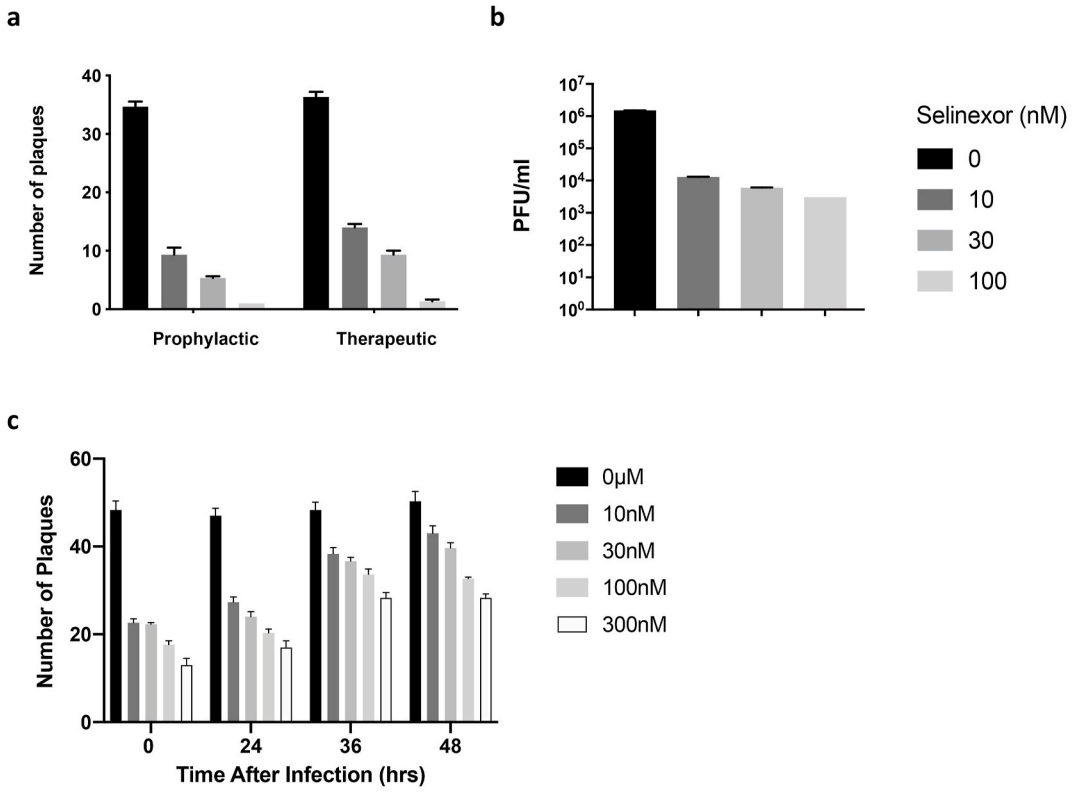


**Fig. 2. Selinexor inhibits SARS-CoV-2 viral replication and shedding *in vitro*.** **a**) Vero E6 cells were pre-treated with selinexor before SARS-CoV-2 infection (left – Prophylactic) or treated with selinexor at the time of infection (right – Therapeutic). Both were incubated with selinexor during infection. Viral load was assessed by plaque assay after 4 days of cell incubation with overlay (Selinexor $CC_{50}$ of Vero E6 Cells at 96 h = 434 nM). **b**) Vero E6 cells were infected with SARS-CoV-2 and viral load was assessed in conditioned media collected after 4 days of incubation. **c**) Vero E6 cells were infected with SARS-CoV-2 at a MOI of 0.01 for 1 h then selinexor was added to overlay media at 0, 24, 36 and 48 h post infection. Viral load was assessed by plaque assay after 4 days of incubation.

### *2.4. Human PBMC studies*

Peripheral blood mononuclear cells (PBMCs) were isolated from whole blood from a SARS-CoV-2 negative donor using Ficoll-Paque™ PLUS Media (GE Health Sciences). Cells were seeded into 96-well plates and selinexor was added to each well at increasing concentrations from 0 to 10000 nM. Then, plates were incubated for 1 h and cells were stimulated with LPS at a final concentration of 1000 ng/ml per well. Cell-free supernatant was collected at 6 h, 16 h, 24 h, and 40 h to analyze IL-2, IFN-γ, IL-6, GM-CSF, TNF-α, IL-1β, IL-8, and IL-10 (reported as pg/ml) according to manufacturer's instructions of individual ELISA assays (R&D Systems).

### *2.5. Statistical analyses*

The $IC_{50}$ values, which indicate the concentration that led to a 50% reduction in cell cytotoxicity, were calculated using a nonlinear regression model with variable slope. Statistical analyses and $IC_{50}$ calculations were performed using GraphPad Prism (version 8.4.3).

## 3. Results

### *3.1. Selinexor mechanism-of-action*

To identify the host and SARS-CoV-2 proteins that are directly modulated by inhibition of XPO1 and could facilitate selinexor-mediated anti-viral activity, we analyzed accessory proteins related to SARS-CoV-2 infection to predict NESs. We determined that human ACE-2 is likely an XPO1 cargo protein after identifying two leucine-rich NESs – one with high affinity ("strong") for amino acids 85–101 (QEIQNLTVKLQLQALQ) and the second with "moderate" for amino acids 529–544 (EAGQKLFNMLRLGKSE) (Table 1). The algorithm also predicted "moderate" NESs in TMPRSS2 and ADAM17, both known to have roles in viral entry. An additional NES, ranked "moderate" was found in the GLTSCR2 protein (amino acids 271–285, EAEKLERQLALPATE), which has been shown to undergo XPO1-mediated translocation from the nucleus to the cytoplasm upon viral infection, and attenuates type I interferon response to support viral replication (Wang et al., 2016). As expected, the algorithm identified the well-studied IκBα NES as "strong" (Table 1). Potential NES peptides were also ranked by the algorithm as "moderate" or "weak" in five of the SARS-CoV-2 proteins (Table 1), as at least three were reported to shuttle between the host cell nucleus and cytoplasm upon viral infection in studies of SARS-CoV (Moshynskyy et al., 2007; Sharma et al., 2011; Timani et al., 2005; You et al., 2007).

We postulated that treatment with selinexor would lead to ACE-2 accumulation within the nucleus, thus protecting the cells from SARS-CoV-2 infection. In order to test if XPO1 inhibition by selinexor affects the subcellular distribution of ACE-2 *in vitro*, Vero E6 cells were treated with selinexor for 24 h and ACE-2 localization was analyzed by immunofluorescence and sub-cellular fractionation. Selinexor treatment induced the nuclear retention of the ACE-2 receptor, while DMSO-treated cells showed membrane bound ACE-2 (Fig. 1A). Immunoblots of sub-cellular fractions showed that XPO1 inhibition by selinexor induced nuclear accumulation of ACE-2, with decreased ACE-2 in the membrane/cytoplasmic fraction, and nearly a 5-fold increase in nuclear protein levels (Fig. 1B and C). Selinexor treatment also led to nuclear accumulation of the well-established XPO1 cargo p53 tumor suppressor protein (Fig. 1B and C). Assessment of total protein levels showed that cells treated with selinexor had an overall reduction in GLTSCR2 and an expected decrease of XPO1 protein (Fig. 1D) (Kashyap et al., 2016; Lee et al., 2020). Importantly, these effects were observed at concentrations

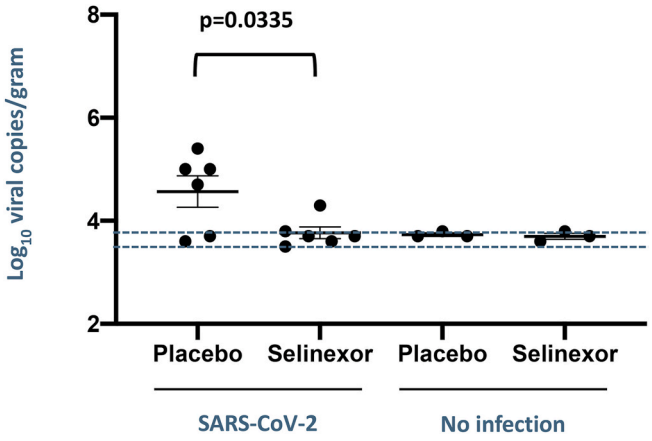


**Fig. 3. Selinexor decreased SARS-CoV-2 viral load in ferret lung tissue.** Levels of viral RNA in the lungs were measured post-mortem on Day 4 by qPCR. Lower limit of detection range is indicated by dashed lines. Data are expressed as mean ± SEM.

that do not affect cell viability as indicated by levels of full-length caspase 3 (Fig. 1D). These results suggest that selinexor could potentially protect host cells from SARS-CoV-2 infection by sequestering ACE-2 in the nucleus to reduce the expression of membrane ACE-2 receptors.

### 3.2. Selinexor inhibits SARS-CoV-2 viral propagation and shedding in vitro

To test the anti-viral effects of selinexor on SARS-CoV-2 infection *in vitro*, Vero E6 cells were incubated with varying concentrations of selinexor starting either 6 h prior (prophylactic) or at the time of viral infection (therapeutic) (Fig. 2A). Both experiments demonstrated that selinexor has potent anti-SARS-CoV-2 activity *in vitro*, with 50% inhibition ($EC_{50}$) of SARS-CoV-2 replication at 10 nM and $EC_{90}$ at 100 nM in the Vero E6 cells. To test the cytotoxic effects of selinexor on Vero E6 cells, the cells were incubated with increasing concentrations of selinexor and the $CC_{50}$ was found to be 434 nM. These results demonstrated that the therapeutic index ([TI] = $CC_{50}/EC_{50}$) of selinexor against SARS-CoV-2 infection in Vero E6 cells is 35.

To test the anti-viral activity of selinexor on uninfected neighboring cells, Vero E6 cells were incubated prophylactically with different concentrations of selinexor starting 6 h prior to infection with SARS-CoV-2 and continuing for the duration of the experiment. This allowed viral shedding of SARS-CoV-2 virus from infected cells into the conditioned media and the infection of other cultured cells in the plate. Four days after the initial infection, the viral load was calculated as plaque forming units (PFU)/ml of conditioned media. The results show that selinexor inhibited SARS-CoV-2 viral shedding and therefore protected the infection of neighboring cells with an $IC_{90} < 10$ nM (Fig. 2B).

To test how long after SARS-CoV-2 viral infection selinexor remains effective inhibiting viral propagation, Vero E6 cells infected with SARS-CoV-2 were treated with selinexor at 0, 24, 36, and 48 h post infection. Assessment of viral load demonstrated that selinexor inhibited SARS-CoV-2 viral propagation *in vitro* even when added up to 48 h after infection (Fig. 2C).

### 3.3. Selinexor demonstrated efficacy against SARS-CoV-2 in ferrets

To assess the *in vivo* therapeutic efficacy of selinexor against SARS-CoV-2 infection, we used a ferret model of viral challenge where animals were infected intranasally with SARS-CoV-2, then treated with either selinexor (5 mg/kg) or placebo (vehicle only) for three days starting 4 h after infection. On day 4 post-SARS-CoV-2 infection, placebo-treated animals had a mean viral RNA of 4.6 $\log_{10}$ viral copies/gram (vc/g) of lung tissue, whereas selinexor-treated animals had a mean of 3.8 vc/g ($p = 0.0335$), with most animals measuring in lower limit of detection of the assay (Fig. 3).

Histopathological analysis of formalin-fixed tissue from the respiratory tracts of animals that had been infected with SARS-CoV-2 showed severe neutrophilic rhinitis with lamina propria necrosis and inflammation in the lamina propria when treated with placebo. Animals treated with selinexor had mild to moderate neutrophilic rhinitis with mild and focal epithelial necrosis that was significantly less severe ($p = 0.0001$) (Fig. 4A–E). The lungs demonstrated inflammation of the bronchial tubes (bronchitis) in infected ferrets treated with placebo, but not in infected ferrets treated with selinexor (Fig. 5A–D). Quantification of pathological changes in the lungs demonstrated that the extent of alveolitis was significantly decreased in selinexor-treated animals with a score of 1.5 out of 3 compared to 2.04 in the vehicle placebo-treated animals ($p = 0.045$) (Fig. 6A). The average severity of alveolitis and bronchitis was also numerically lower in the selinexor-treated animals, but the difference did not reach statistical significance (Fig. 6B and C).

### 3.4. Selinexor inhibits inflammatory cytokine expression by LPS-stimulated human PBMCs

As described above, selinexor as well as other SINE compounds force the nuclear retention and functional activation of IκB and other anti-inflammatory proteins, leading to attenuation of NF-κB and other pro-inflammatory transcription factors (Widman et al., 2018; Wu et al., 2018). To further evaluate the anti-inflammatory effects of selinexor, PBMCs from human volunteers were isolated, stimulated with LPS, and incubated with increasing concentrations of selinexor. Cell free supernatants were collected at 6, 16, 24, and 40 h post-incubation and assayed by ELISA for selected pro- and anti-inflammatory cytokines. Compared with vehicle, selinexor inhibited production of IL-1β, IL-6, TNF-α, IL-10, and IFN-γ at each time point. In addition, production of GM-CSF and IL-8 showed moderate decreases with the highest dose of selinexor at later timepoints (Fig. 7).

## 4. Discussion

Selinexor is one of several SINE drug molecules that binds covalently to cysteine 528 in the cargo binding pocket of XPO1 and inhibits its ability to facilitate nuclear export, leading to the accumulation of XPO1 and its cargo proteins in the nucleus. In addition to proteins at the epicenter of inflammation, cell-cycle and cell survival pathways, the more than 200 XPO1 cargo proteins also include viral proteins and accessory host proteins that enable efficient viral infection, replication, suppression of host innate immunity. In this report, we focused on the XPO1 inhibitor selinexor and demonstrated its direct anti-viral activity against SARS-CoV-2, and indirect anti-inflammatory activities.

The role of XPO1 in SARS-CoV/SARS-CoV-2 replication and pathogenesis has been examined previously (Freundt et al., 2009; Jiang et al., 2020; Konno et al., 2020; Li et al., 2020; Moshynskyy et al., 2007; Sharma et al., 2011; Shi et al., 2014; Timani et al., 2005; You et al., 2007). ORF3b, ORF9b and the nucleocapsid protein have all been shown to localize to the cell nucleus and undergo XPO1-mediated nuclear export (Sharma et al., 2011) (Freundt et al., 2009) (Timani et al., 2005; You et al., 2007). In addition, the SARS-CoV ORF3b, ORF9b and nucleocapsid proteins, are β-interferon antagonists, blocking the innate immune response which is activated to combat viral infection (Freundt et al., 2009; Kopecky-Bromberg et al., 2007). Recently, the SARS-CoV-2 ORF3b, ORF9b and the nucleocapsid proteins have also been shown to counteract the innate immune response (Jiang et al., 2020; Konno et al., 2020; Li et al., 2020).

Additionally, the role of XPO1 in SARS-CoV/SARS-CoV-2 replication and pathogenesis is not limited to direct interactions with viral proteins, as XPO1 was recently identified as one of four hub proteins suggested as candidates for targeted COVID-19 therapies because of their

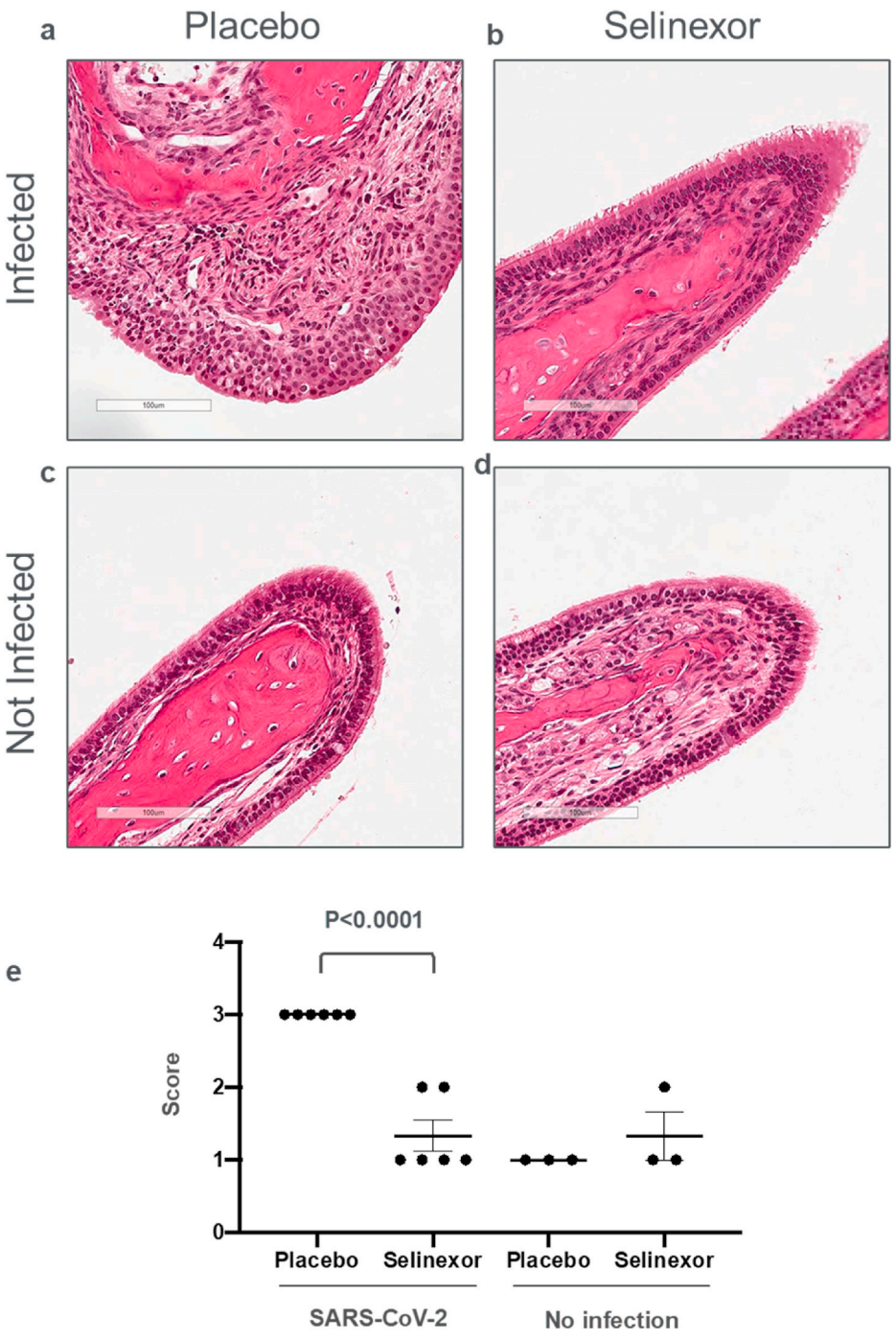


**Fig. 4. Selinexor protects from pathological changes associated with SARS-CoV-2 infection in nasal turbinates.** Histopathological analysis in formalin-fixed tissue demonstrates inflammation of the nasal turbinates (rhinitis) in infected ferrets treated with placebo (**a**), but not in infected ferrets treated with selinexor (**b**) or uninfected animals (**c**, **d**). Inflammation is seen as infiltrates of inflammatory cells (leukocytes) in the lamina propria/submucosa (epithelium) of the nasal turbinates with associated edema and prominent (dilated) blood vessels. **e**) Quantification based on 5 sections from 6 animals to determine the severity of rhinitis (score details described in methods). Data are expressed as mean ± SEM.

downstream targets, specifically GSK3B, SMAD3, PARP1, and IκB (Zhu et al., 2020). This is in alignment with a recent *in vitro* study showing that another SINE compound, verdinexor, inhibited protein-protein interactions between SARS-CoV-2 proteins and human host proteins, suggesting that it may interfere with viral propagation and could be a potential treatment for COVID-19 (Gordon et al., 2020).

Our results demonstrated that at least four of the SARS-CoV-2 proteins (nucleocapsid, ORF3b, ORF9b and the spike protein) contain predicted NESs, and three of these have been experimentally validated by others to be XPO1 cargos (Table 1). Similarly, we found that five of the human host proteins we tested contain NESs, including GLTSCR2 and Iκb, which have been previously experimentally validated (Table 1). ACE-2, the functional receptor for the SARS-CoV-2 spike glycoprotein contains two predicted NESs (Table 1). Our studies confirmed that XPO1 inhibition by selinexor induced nuclear retention of ACE-2 and reduced its cell surface localization (Fig. 1), providing experimental evidence to support ACE-2 as an XPO1 cargo protein. Reduction of ACE-2 membranal expression diminishes SARS-CoV-2 viral infection, as was demonstrated in ACE-2 knockout mice (Kuba et al., 2005). Therefore, our findings that selinexor inhibited SARS-CoV-2 viral replication and shedding *in vitro* (Fig. 2) are consistent with a mechanism by which selinexor-mediated XPO1-inhibition leads to a reduction in the cellular membrane fraction of ACE-2, which helps to protect from viral infection. We showed that selinexor inhibited viral infection when given prophylactically, at the time of viral infection and also up to 24 h following cell infection (Fig. 2). These results suggest that selinexor can protect healthy tissue from infection in an infected individual. Importantly, selinexor levels required to block viral replication are not cytotoxic, with

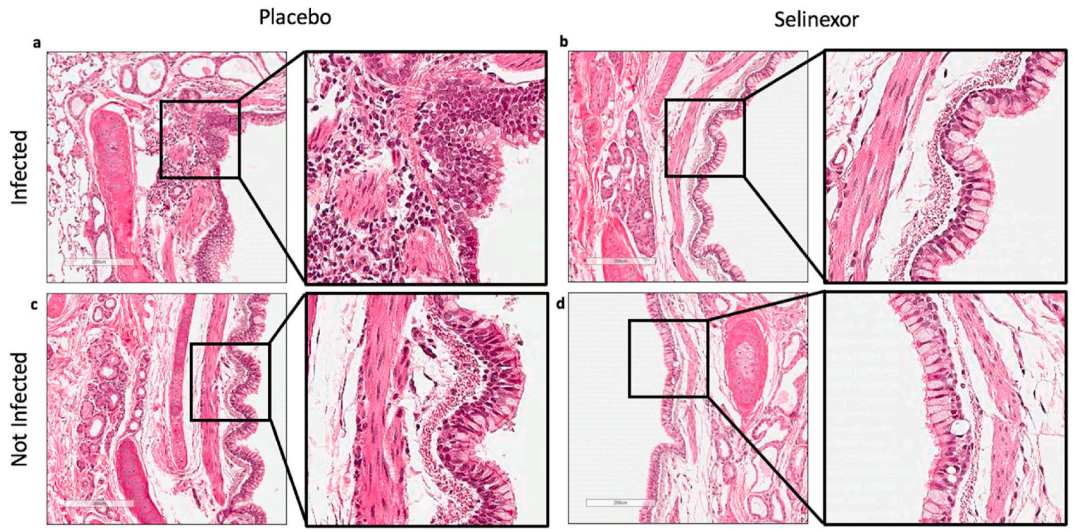


**Fig. 5. Selinexor protects from pathological changes associated with SARS-CoV-2 lung infection.** Histopathological analysis in formalin-fixed tissue demonstrates inflammation of the bronchial tubes (bronchitis) in infected ferrets treated with placebo (**a**), but not in infected ferrets treated with selinexor (**b**) or uninfected animals (**c**, **d**). Insets show higher magnifications of indicated fields.

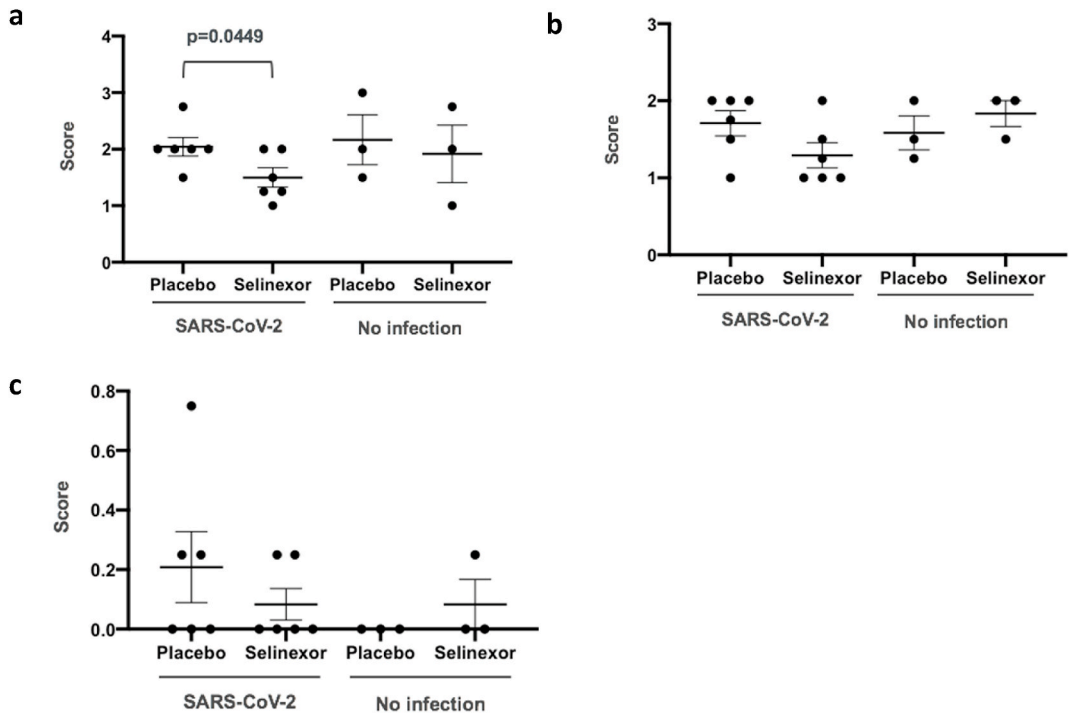


**Fig. 6. Quantitative assessment of selinexor effects on alveolitis and bronchitis after SARS-CoV-2 lung infection.** Histopathological analysis was performed on formalin-fixed lungs. Tissues were analyzed for the **a**) extent and **b**) severity of alveolitis, and severity of **c**) bronchitis. Quantification based on 5 sections from 6 animals. Data are expressed as mean ± SEM.

a therapeutic index of 35 (Fig. 2).

Alveolar injury and interstitial inflammation in COVID-19 patients is induced through a "cytokine storm" in the infected target tissue (Gavriatopoulou et al., 2020; Mehta et al., 2020). This reaction occurs when dendritic cells and alveolar macrophages phagocytose the virus-infected epithelial cells undergoing apoptosis, resulting in T-cell responses that activate the innate and adaptive immune mechanisms (Channappanavar et al., 2014). Also, during the cytokine storm, proinflammatory cytokine and chemokine levels, such as TNF-α, IL-1β, IL-6, are increased, further propagating the extensive hemophagocytosis (Gavriatopoulou et al., 2020). In addition to inhibiting cytokines associated with the COVID-19 cytokine storm, our study also demonstrated that selinexor protected from pathological changes in lung and nasal tissue associated with the cytokine storm caused by SARS-CoV-2 infection. These results strengthen previous findings of direct inhibition of inflammation and cytokine secretion by SINE compounds in animal models of traumatic brain injury (Tajiri et al., 2016), LPS-induced septic shock (Wu et al., 2018), influenza (Perwitasari et al., 2014), and *in vitro* viral infection studies (Jorquera et al., 2019; Perwitasari et al., 2014; Widman et al., 2018). It is likely that the combination of anti-viral and anti-inflammatory activities of selinexor provided protection from the SARS-CoV-2 induced tissue damage.

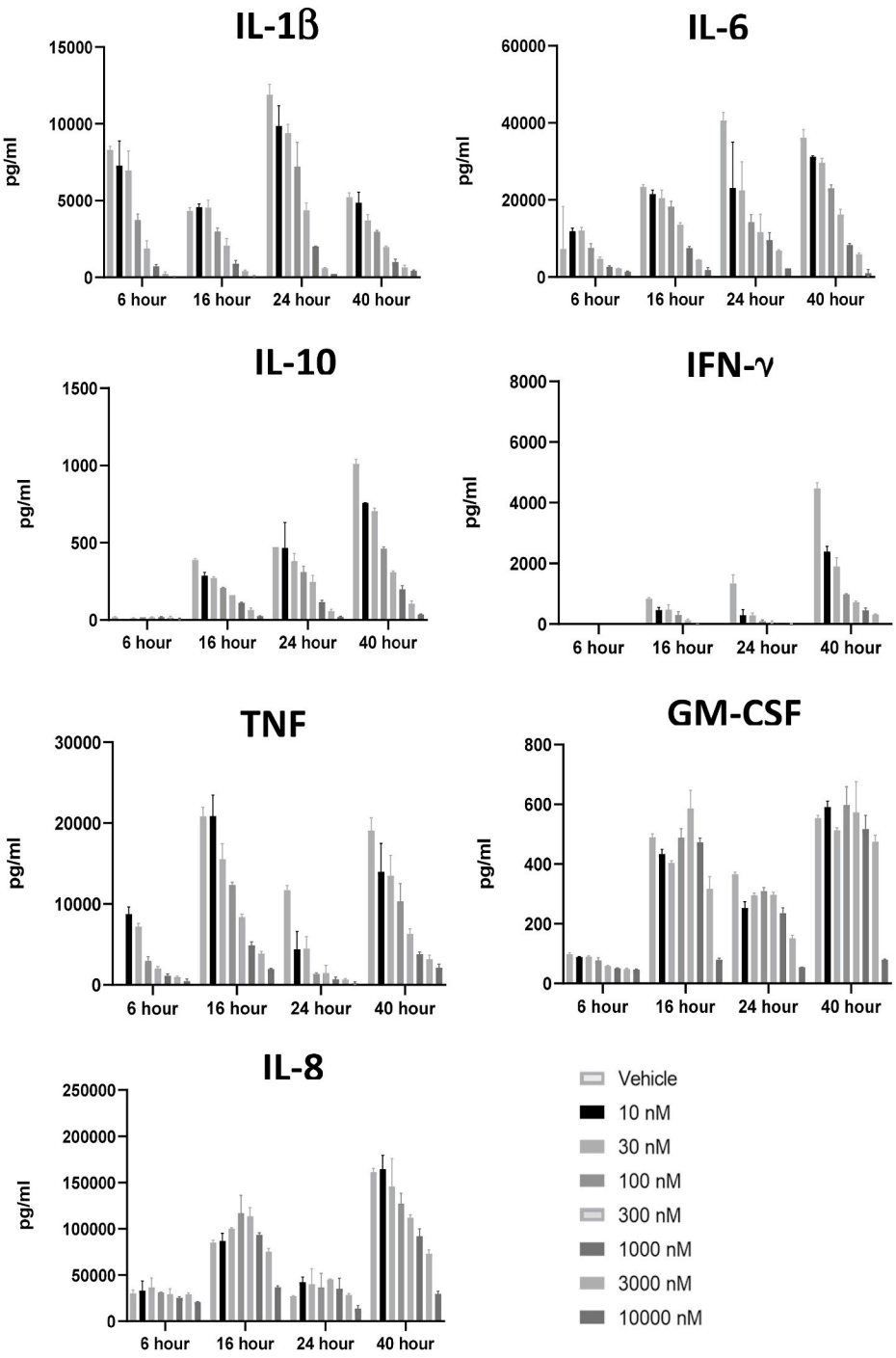


**Fig. 7. Selinexor diminishes inflammatory cytokine levels associated with SARS-CoV-2 infection in human cells.** Human peripheral blood mononuclear cells were incubated with LPS (1000 ng/ml) and increasing concentrations of selinexor for 6, 16, 24, and 40 h. Supernatant was collected and analyzed by individual ELISAs. Data are expressed as mean ± SEM.

The ACE-2 receptor is ubiquitously expressed in many organs including lungs, heart, kidney, testis, gut, and brain (Saponaro et al., 2020). One of its roles is to catalyze the formation of angiotensin-(1–7) through either degradation of angiotensin II or conversion of angiotensin I into angiotensin-(1–9), which in turn, is converted to angiotensin-(1–7) (Verdecchia et al., 2020). Through this process, ACE-2 receptors protect tissue from vasoconstriction, fibrosis, enhanced inflammation, pulmonary damage, and thrombosis that occurs when $AT_1$ receptors bind angiotensin II (Verdecchia et al., 2020). As we have provided evidence that ACE-2 is an XPO1 cargo, it is worth discussing the potential clinical outcome of the membranal reduction of ACE-2 in selinexor treated patients. *In vivo* studies show mild acute lung injury in ACE-2 knockout mice (Kuba et al., 2005). Unlike the ACE-2 knockout, the effects of selinexor on the membranal expression of ACE-2 are milder and transient. Selinexor treatment reduced membranal and cytoplasmic ACE-2 without completely depleting it from the cell membrane (Fig. 1). In addition, preclinical and clinical use of selinexor demonstrated maximal activity in the first 48 h after drug dosing, and human selinexor treatment for a number of non-viral indications demonstrated tolerability with no hyperactivation of $AT_1$ receptors (Abdul Razak et al., 2016; Grosicki et al., 2020; Kalakonda et al., 2020).

Taken together, XPO1 inhibition, including the reduction of

a

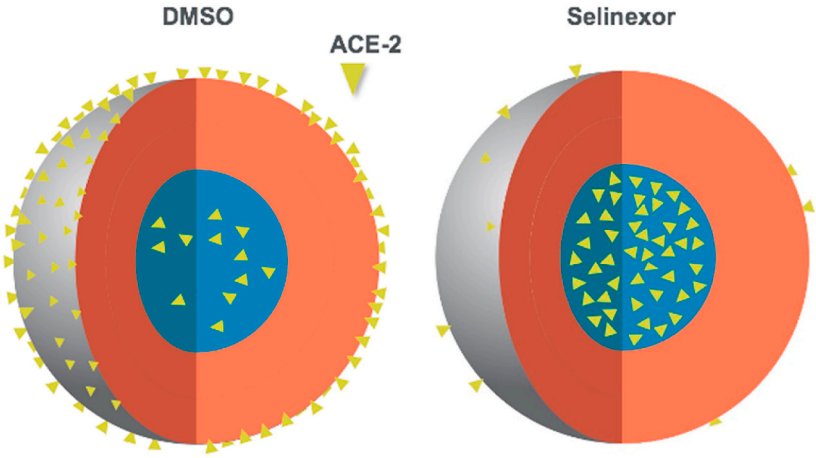


b

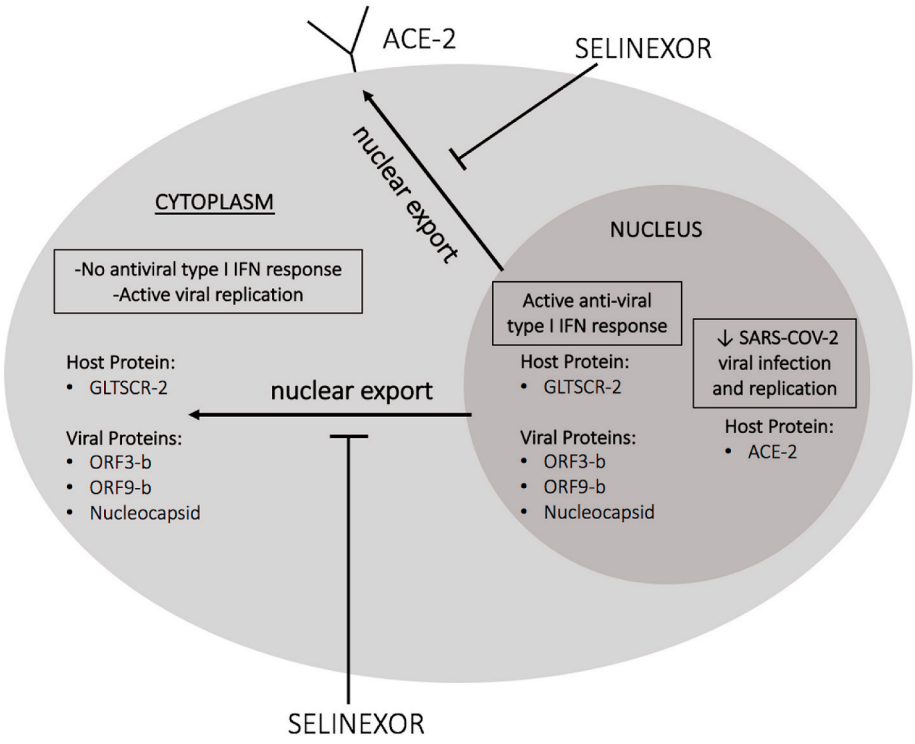


**Fig. 8. Blocking nuclear export inhibits SARS-CoV-2 infection, replication and viral propagation. a)** Selinexor treatment blocks nuclear export and induces nuclear localization of the ACE-2 protein. Our results demonstrate that selinexor induces significant retention of ACE-2 in the cell nucleus while a small portion remained on the cell surface as seen in Fig. 1a and b. The reduction in ACE-2 on the cell surface confers protection from SARS-CoV-2 infection. **b)** A schematic model demonstrates how inhibition of nuclear export protects cells from SARS-CoV-2 infection by: reducing membranal presentation of ACE-2, blocking the cytoplasmic shuttling of the host protein GLTSCR2, (Wang et al., 2016), and sequestering the viral proteins ORF3b (Freundt et al., 2009), ORF9b (Moshynskyy et al., 2007; Sharma et al., 2011), and the nucleocapsid protein (Timani et al., 2005; You et al., 2007) in the nucleus. This allows for the activation of the innate immune response and the production of the type I interferons.

membranal ACE-2 receptor (Fig. 8A), exerts therapeutic effects due to the inhibition of viral infection, activation of the type I interferon response, and anti-inflammatory activity (Fig. 8B), blocking viral infection, replication, and propagation of SARS-CoV-2. Future studies will directly examine the role of additional host and viral proteins in SARS-CoV-2 infection and the effects of selinexor on their functions in order to identify combinations with other drugs that may synergize and enhance selinexor activity for the potential use of SINE compounds, including selinexor, in the clinic.

## Funding

This study was supported by Karyopharm Therapeutics Inc.

## Acknowledgements

The authors would like to thank Susie Harrington, Corporate Design Lead at Karyopharm, for graphical assistance. JetPub Scientific Communications, LLC supported by funding from Karyopharm, provided drafts and editorial assistance to the authors during preparation of this manuscript.

## References

Abdul Razak, A.R., Mau-Soerensen, M., Gabrail, N.Y., Gerecitano, J.F., Shields, A.F., Unger, T.J., Saint-Martin, J.R., Carlson, R., Landesman, Y., McCauley, D., Rashal, T., Lassen, U., Kim, R., Stayner, L.A., Mirza, M.R., Kauffman, M., Shacham, S., Mahipal, A., 2016. First-in-class, first-in-human phase I study of selinexor, a selective

inhibitor of nuclear export, in patients with advanced solid tumors. J. Clin. Oncol. 34, 4142–4150. https://doi.org/10.1200/JCO.2015.65.3949.
Cao, Y., Liu, X., De Clercq, E., 2009. Cessation of HIV-1 transcription by inhibiting regulatory protein Rev- mediated RNA transport. Curr. HIV Res. 7, 101–108. https://doi.org/10.2174/157016209787048564.
Channappanavar, R., Zhao, J., Perlman, S., 2014. T cell-mediated immune response to respiratory coronaviruses. Immunol. Res. 59, 118–128. https://doi.org/10.1007/s12026-014-8534-z.
Corman, V.M., Landt, O., Kaiser, M., Molenkamp, R., Meijer, A., Chu, D.K., Bleicker, T., Brünink, S., Schneider, J., Schmidt, M.L., Mulders, D.G., Haagmans, B.L., van der Veer, B., van den Brink, S., Wijsman, L., Goderski, G., Romette, J.-L., Ellis, J., Zambon, M., Peiris, M., Goossens, H., Reusken, C., Koopmans, M.P., Drosten, C., 2020. Detection of 2019 novel coronavirus (2019-nCoV) by real-time RT-PCR. Euro Surveill. 25 (3), 2000045 https://doi.org/10.2807/1560-7917.ES.2020.25.3.2000045.
Freundt, E.C., Yu, L., Park, E., Lenardo, M.J., Xu, X.-N., 2009. Molecular determinants for subcellular localization of the severe acute respiratory syndrome coronavirus open reading frame 3b protein. J. Virol. 83 (13), 6631–6640. https://doi.org/10.1128/jvi.00367-09.
Gandhi, R.T., Lynch, J.B., del Rio, C., 2020. Mild or moderate Covid-19. N. Engl. J. Med. 383 (18), 1757–1766. https://doi.org/10.1056/nejmcp2009249.
Gavriatopoulou, M., Korompoki, E., Fotiou, D., Ntanasis-Stathopoulos, I., Psaltopoulou, T., Kastritis, E., Terpos, E., Dimopoulos, M.A., 2020. Organ-specific manifestations of COVID-19 infection. Clin. Exp. Med. 20 (4), 493–506. https://doi.org/10.1007/s10238-020-00648-x.
Gordon, D.E., Jang, G.M., Bouhaddou, M., Xu, J., Obernier, K., O'Meara, M.J., Guo, J.Z., Swaney, D.L., Tummino, T.A., Huettenhain, R., Kaake, R.M., Richards, A.L., Tutuncuoglu, B., Foussard, H., Batra, J., Haas, K., Modak, M., Kim, M., Haas, P., Polacco, B.J., Braberg, H., Fabius, J.M., Eckhardt, M., Soucheray, M., Bennett, M.J., Cakir, M., McGregor, M.J., Li, Q., Naing, Z.Z.C., Zhou, Y., Peng, S., Kirby, I.T., Melnyk, J.E., Chorba, J.S., Lou, K., Dai, S.A., Shen, W., Shi, Y., Zhang, Z., Barrio-Hernandez, I., Memon, D., Hernandez-Armenta, C., Mathy, C.J.P., Perica, T., Pilla, K. B., Ganesan, S.J., Saltzberg, D.J., Ramachandran, R., Liu, X., Rosenthal, S.B., Calviello, L., Venkataramanan, S., Liboy-Lugo, J., Lin, Y., Wankowicz, S.A., Bohn, M., Sharp, P.P., Trenker, R., Young, J.M., Cavero, D.A., Hiatt, J., Roth, T.L., Rathore, U., Subramanian, A., Noack, J., Hubert, M., Roesch, F., Vallet, T., Meyer, B., White, K.M., Miorin, L., Rosenberg, O.S., Verba, K.A., Agard, D., Ott, M., Emerman, M., Ruggero, D., García-Sastre, A., Jura, N., von Zastrow, M., Taunton, J., Ashworth, A., Schwartz, O., Vignuzzi, M., d'Enfert, C., Mukherjee, S., Jacobson, M., Malik, H.S., Fujimori, D.G., Ideker, T., Craik, C.S., Floor, S., Fraser, J.S., Gross, J., Sali, A., Kortemme, T., Beltrao, P., Shokat, K., Shoichet, B.K., Krogan, N.J., 2020. A SARS-CoV-2-Human Protein-protein Interaction Map reveals Drug Targets and potential Drug-Repurposing, March 27, 2020. bioRxiv. https://doi.org/10.1101/2020.03.22.002386, 2020.
Grosicki, S., Simonova, M., Spicka, I., Pour, L., Kriachok, I., Gavriatopoulou, M., Pylypenko, H., Auner, H.W., Leleu, X., Doronin, V., Usenko, G., Bahlis, N.J., Hajek, R., Benjamin, R., Dolai, T.K., Sinha, D.K., Venner, C.P., Garg, M., Gironella, M., Jurczyszyn, A., Robak, P., Galli, M., Wallington-Beddoe, C., Radinoff, A., Salogub, G., Stevens, D.A., Basu, S., Liberati, A.M., Quach, H., Goranova-Marinova, V.S., Bila, J., Katodritou, E., Oliynyk, H., Korenkova, S., Kumar, J., Jagannath, S., Moreau, P., Levy, M., White, D., Gatt, M.E., Facon, T., Mateos, M.V., Cavo, M., Reece, D., Anderson, L.D., Saint-Martin, J.-R., Jeha, J., Joshi, A.A., Chai, Y., Li, L., Peddagali, V., Arazy, M., Shah, J., Shacham, S., Kauffman, M.G., Dimopoulos, M.A., Richardson, P.G., Delimpasi, S., 2020. Once-per-week selinexor, bortezomib, and dexamethasone versus twice-per-week bortezomib and dexamethasone in patients with multiple myeloma (BOSTON): a randomised, open-label, phase 3 trial. Lancet 396, 1563–1573. https://doi.org/10.1016/S0140-6736(20)32292-3.
Heurich, A., Hofmann-Winkler, H., Gierer, S., Liepold, T., Jahn, O., Pohlmann, S., 2014. TMPRSS2 and ADAM17 cleave ACE2 differentially and only proteolysis by TMPRSS2 augments entry driven by the severe acute respiratory syndrome coronavirus spike protein. J. Virol. 88, 1293–1307. https://doi.org/10.1128/jvi.02202-13.
Hyun, H.W., Ko, A.R., Kang, T.C., 2016. Mitochondrial translocation of high mobility group box 1 facilitates LIM kinase 2-mediated programmed necrotic neuronal death. Front. Cell. Neurosci. 10 https://doi.org/10.3389/fncel.2016.00099.
Ingraham, N.E., Lotfi-Emran, S., Thielen, B.K., Techar, K., Morris, R.S., Holtan, S.G., Dudley, R.A., Tignanelli, C.J., 2020. Immunomodulation in COVID-19. Lancet. Respir. Med 8 (6), 544–546. https://doi.org/10.1016/S2213-2600(20)30226-5.
Jiang, H. wei, Zhang, H. nan, Meng, Q. feng, Xie, J., Li, Y., Chen, H., Zheng, Y. xiao, Wang, X. ning, Qi, H., Zhang, J., Wang, P.H., Han, Z.G., Tao, S. ce, 2020. SARS-CoV-2 Orf9b suppresses type I interferon responses by targeting TOM70. Cell. Mol. Immunol. 17, 998–1000. https://doi.org/10.1038/s41423-020-0514-8.
Johnson, Connie, Van Antwerp, Daniel, Hope, Thomas J., 1999. An N-terminal nuclear export signal is required for the nucleocytoplasmic shuttling of IkappaBalpha. EMBO Journal 18 (23), 6682–6693. https://doi.org/10.1093/emboj/18.23.6682.
Jorquera, P.A., Mathew, C., Pickens, J., Williams, C., Luczo, J.M., Tamir, S., Ghildyal, R., Tripp, R.A., 2019. Verdinexor (KPT-335), a selective inhibitor of nuclear export, reduces respiratory syncytial virus replication. J. Virol 93 (4), e01684–18. https://doi.org/10.1128/jvi.01684-18.
Kalakonda, N., Maerevoet, M., Cavallo, F., Follows, G., Goy, A., Vermaat, J.S.P., Casasnovas, O., Hamad, N., Zijlstra, J.M., Bakhshi, S., Bouabdallah, R., Choquet, S., Gurion, R., Hill, B., Jaeger, U., Sancho, J.M., Schuster, M., Thieblemont, C., De la Cruz, F., Egyed, M., Mishra, S., Offner, F., Vassilakopoulos, T.P., Warzocha, K., McCarthy, D., Ma, X., Corona, K., Saint-Martin, J.R., Chang, H., Landesman, Y., Joshi, A., Wang, H., Shah, J., Shacham, S., Kauffman, M., Van Den Neste, E., Canales, M.A., 2020. Selinexor in patients with relapsed or refractory diffuse large B-cell lymphoma (SADAL): a single-arm, multinational, multicentre, open-label, phase 2 trial. Lancet Haematol 7 (7), e511–e522. https://doi.org/10.1016/S2352-3026(20)30120-4.
Kashyap, T., Argueta, C., Aboukameel, A., Unger, T.J., Klebanov, B., Mohammad, R.M., Muqbil, I., Azmi, A.S., Drolen, C., Senapedis, W., Lee, M., Kauffman, M., Shacham, S., Landesman, Y., 2016. Selinexor, a Selective Inhibitor of Nuclear Export (SINE) compound, acts through NF-κB deactivation and combines with proteasome inhibitors to synergistically induce tumor cell death. Oncotarget 7 (48), 78883–78895. https://doi.org/10.18632/oncotarget.12428.
Konno, Y., Kimura, I., Uriu, K., Fukushi, M., Irie, T., Koyanagi, Y., Sauter, D., Gifford, R. J., Nakagawa, S., Sato, K., 2020. SARS-CoV-2 ORF3b is a potent interferon antagonist whose activity is increased by a naturally occurring elongation variant. Cell Rep. 32 (12), 108185. https://doi.org/10.1016/j.celrep.2020.108185.
Kopecky-Bromberg, S.A., Martínez-Sobrido, L., Frieman, M., Baric, R.A., Palese, P., 2007. Severe acute respiratory syndrome coronavirus open reading frame (ORF) 3b, ORF 6, and nucleocapsid proteins function as interferon antagonists. J. Virol. 81, 548–557. https://doi.org/10.1128/jvi.01782-06.
Kuba, K., Imai, Y., Rao, S., Gao, H., Guo, F., Guan, B., Huan, Y., Yang, P., Zhang, Y., Deng, W., Bao, L., Zhang, B., Liu, G., Wang, Z., Chappell, M., Liu, Y., Zheng, D., Leibbrandt, A., Wada, T., Slutsky, A.S., Liu, D., Qin, C., Jiang, C., Penninger, J.M., 2005. A crucial role of angiotensin converting enzyme 2 (ACE2) in SARS coronavirus-induced lung injury. Nat. Med. 11, 875–879. https://doi.org/10.1038/nm1267.
la Cour, T., Kiemer, L., Mølgaard, A., Gupta, R., Skriver, K., Brunak, S., 2004. Analysis and prediction of leucine-rich nuclear export signals. Protein Eng. Des. Sel. 17, 527–536. https://doi.org/10.1093/protein/gzh062.
Lai, C.C., Shih, T.P., Ko, W.C., Tang, H.J., Hsueh, P.R., 2020. Severe acute respiratory syndrome coronavirus 2 (SARS-CoV-2) and coronavirus disease-2019 (COVID-19): the epidemic and the challenges. Int. J. Antimicrob. Agents 55 (3), 105924–105932. https://doi.org/10.1016/j.ijantimicag.2020.105924.
Laise, P., Bosker, G., Sun, X., Shen, Y., Douglass, E.F., Karan, C., Realubit, R.B., Pampou, S., Califano, A., Alvarez, M.J., 2020. The host cell ViroCheckpoint: Identification and pharmacologic targeting of novel mechanistic determinants of Coronavirus-mediated Hijacked cell states. Prepr. Serv. Biol. May 17, 2020, 1–20. https://doi.org/10.1101/2020.05.12.091256 bioRxiv.
Lee, Y., Baumhardt, J.M., Pei, J., Chook, Y.M., Grishin, N.V., 2020. pCRM1exportome: database of predicted CRM1-dependent Nuclear Export Signal (NES) motifs in cancer-related genes. Bioinformatics 36, 961–963. https://doi.org/10.1093/bioinformatics/btz657.
Li, C.C., Dong, H.J., Wang, P., Meng, W., Chi, X.J., Han, S.C., Ning, S., Wang, C., Wang, X. J., 2017. Cellular protein GLTSCR2: a valuable target for the development of broad-spectrum antivirals. Antivir. Res. 142, 1–11. https://doi.org/10.1016/j.antiviral.2017.03.004.
Li, J.Y., Liao, C.H., Wang, Q., Tan, Y.J., Luo, R., Qiu, Y., Ge, X.Y., 2020. The ORF6, ORF8 and nucleocapsid proteins of SARS-CoV-2 inhibit type I interferon signaling pathway. Virus Res. 286 https://doi.org/10.1016/j.virusres.2020.198074.
Mehta, P., McAuley, D.F., Brown, M., Sanchez, E., Tattersall, R.S., Manson, J.J., 2020. COVID-19: consider cytokine storm syndromes and immunosuppression. Lancet 395, 1033–1034. https://doi.org/10.1016/S0140-6736(20) 30628–0.
Moshynskyy, I., Viswanathan, S., Vasilenko, N., Lobanov, V., Petric, M., Babiuk, L.A., Zakhartchouk, A.N., 2007. Intracellular localization of the SARS coronavirus protein 9b: evidence of active export from the nucleus. Virus Res. 127, 116–121. https://doi.org/10.1016/j.virusres.2007.03.011.
Muller, P.A.J., Sluis, De, Van, B., Groot, A.J., Verbeek, D., Vonk, W.I.M., Maine, G.N., Burstein, E., Wijmenga, C., Vooijs, M., Reits, E., Klomp, L.W.J., 2009. Nuclear-cytosolic transport of COMMD1 regulates NF-κB and HIF-1 activity. Traffic 10, 514–527. https://doi.org/10.1111/j.1600-0854.2009.00892.x.
Paragas, J., Talon, J., O'Neill, R.E., Anderson, D.K., García, Sastre A., Palese, P., 2001. Influenza B and C virus NEP (NS2) proteins possess nuclear export activities. J. Virol. 75, 7375–7383. https://doi.org/10.1128/jvi.75.16.7375-7383.2001.
Perwitasari, O., Johnson, S., Yan, X., Howerth, E., Shacham, S., Landesman, Y., Baloglu, E., McCauley, D., Tamir, S., Tompkins, S.M., Tripp, R.A., 2014. Verdinexor, a novel selective inhibitor of nuclear export, reduces influenza A virus replication in vitro and. Vivo. J. Virol 88, 10228–10243. https://doi.org/10.1128/jvi.01774-14.
Perwitasari, O., Johnson, S., Yan, X., Register, E., Crabtree, J., Gabbard, J., Howerth, E., Shacham, S., Carlson, R., Tamir, S., Tripp, R.A., 2016. Antiviral efficacy of verdinexor in vivo in two animal models of influenza A virus infection. PLoS One 11, e0167221. https://doi.org/10.1371/journal.pone.0167221.
Prieto, G., Fullaondo, A., Rodriguez, J.A., 2014. Prediction of Nuclear Export Signals using Weighted Regular Expressions (Wregex), 30, pp. 1220–1227. https://doi.org/10.1093/bioinformatics/btu016.
Prüfer, K., Barsony, J., 2002. Retinoid X Receptor dominates the nuclear import and export of the unliganded vitamin D receptor. Mol. Endocrinol. 16, 1738–1751. https://doi.org/10.1210/me.2001-0345.
Saponaro, F., Rutigliano, G., Sestito, S., Bandini, L., Storti, B., Bizzarri, R., Zucchi, R., 2020. ACE2 in the era of SARS-CoV-2: controversies and novel perspectives. Front. Mol. Biosci 7, 588618. https://doi.org/10.3389/fmolb.2020.588618.
Saribas, A.S., Datta, P.K., Safak, M., 2020. A comprehensive proteomics analysis of JC virus Agnoprotein-interacting proteins: agnoprotein primarily targets the host proteins with coiled-coil motifs. Virology 540, 104–118. https://doi.org/10.1016/j.virol.2019.10.005.
Sharma, K., Åkerström, S., Sharma, A.K., Chow, V.T.K., Teow, S., Abrenica, B., Booth, S. A., Booth, T.F., Mirazimi, A., Lal, S.K., 2011. SARS-CoV 9b protein diffuses into nucleus, undergoes active Crm1 mediated nucleocytoplasmic export and triggers apoptosis when retained in the nucleus. PLoS One 6 (5), e19436. https://doi.org/10.1371/journal.pone.0019436.

Shereen, M.A., Khan, S., Kazmi, A., Bashir, N., Siddique, R., 2020. COVID-19 infection: origin, transmission, and characteristics of human coronaviruses. J. Adv. Res. 24, 91–98. https://doi.org/10.1016/j.jare.2020.03.005.

Shi, C.-S., Qi, H.-Y., Boularan, C., Huang, N.-N., Abu-Asab, M., Shelhamer, J.H., Kehrl, J. H., 2014. SARS-coronavirus open reading frame-9b suppresses innate immunity by targeting mitochondria and the MAVS/TRAF3/TRAF6 signalosome. J. Immunol. 193, 3080–3089. https://doi.org/10.4049/jimmunol.1303196.

Sun, Q., Carrasco, Y.P., Hu, Y., Guo, X., Mirzaei, H., Macmillan, J., Chook, Y.M., 2013. Nuclear export inhibition through covalent conjugation and hydrolysis of Leptomycin B by CRM1. Proc. Natl. Acad. Sci. U. S. A 110, 1303–1308. https://doi.org/10.1073/pnas.1217203110.

Tajiri, N., De La Peña, I., Acosta, S.A., Kaneko, Y., Tamir, S., Landesman, Y., Carlson, R., Shacham, S., Borlongan, C.V., 2016. A nuclear attack on traumatic brain injury: sequestration of cell death in the nucleus. CNS Neurosci. Ther. 22, 306–315. https://doi.org/10.1111/cns.12501.

Timani, K.A., Liao, Q., Ye, Linbai, Zeng, Y., Liu, J., Zheng, Y., Ye, Li, Yang, X., Lingbao, K., Gao, J., Zhu, Y., 2005. Nuclear/nucleolar localization properties of C-terminal nucleocapsid protein of SARS coronavirus. Virus Res. 114, 23–34. https://doi.org/10.1016/j.virusres.2005.05.007.

Uddin, M.H., Zonder, J.A., Azmi, A.S., 2020. Exportin 1 inhibition as antiviral therapy. Drug Discov. Today 25 (10), 1775–1781. https://doi.org/10.1016/j.drudis.2020.06.014.

Umemoto, T., Fujiki, Y., 2012. Ligand-dependent nucleo-cytoplasmic shuttling of peroxisome proliferator-activated receptors, PPARα and PPARγ. Gene Cell. 17, 576–596. https://doi.org/10.1111/j.1365-2443.2012.01607.x.

Verdecchia, P., Cavallini, C., Spanevello, A., Angeli, F., 2020. The pivotal link between ACE2 deficiency and SARS-CoV-2 infection. Eur. J. Intern. Med. 76, 14–20. https://doi.org/10.1016/j.ejim.2020.04.037.

Wang, P., Meng, W., Han, S.C., Li, C.C., Wang, Xiao Jun, Wang, Xiao Jia, 2016. The nucleolar protein GLTSCR2 is required for efficient viral replication. Sci. Rep. 6 https://doi.org/10.1038/srep36226.

Widman, D.G., Gornisiewicz, S., Shacham, S., Tamir, S., 2018. In vitro toxicity and efficacy of verdinexor, an exportin 1 inhibitor, on opportunistic viruses affecting immunocompromised individuals. PLoS One 13 (10), e0200043. https://doi.org/10.1371/journal.pone.0200043.

Wu, M., Gui, H., Feng, Z., Xu, H., Li, G., Li, M., Chen, T., Wu, Y., Huang, J., Bai, Z., Li, Y., Pan, J., Wang, J., Zhou, H., 2018. KPT-330, a potent and selective CRM1 inhibitor, exhibits anti-inflammation effects and protection against sepsis. Biochem. Biophys. Res. Commun. 503, 1773–1779. https://doi.org/10.1016/j.bbrc.2018.07.112.

You, J.H., Reed, M.L., Hiscox, J.A., 2007. Trafficking motifs in the SARS-coronavirus nucleocapsid protein. Biochem. Biophys. Res. Commun. 358, 1015–1020. https://doi.org/10.1016/j.bbrc.2007.05.036.

Zhou, Y., Hou, Y., Shen, J., Huang, Y., Martin, W., Cheng, F., 2020. Network-based drug repurposing for novel coronavirus 2019-nCoV/SARS-CoV-2. Cell Discov. 6, 1–18. https://doi.org/10.1038/s41421-020-0153-3.

Zhu, N., Zhang, D., Wang, W., Li, X., Yang, B., Song, J., Zhao, X., Huang, B., Shi, W., Lu, R., Niu, P., Zhan, F., Ma, X., Wang, D., Xu, W., Wu, G., Gao, G.F., Tan, W., 2020. A novel coronavirus from patients with pneumonia in China, 2019. N. Engl. J. Med. 382, 727–733. https://doi.org/10.1056/nejmoa2001017.